AD-A177 878 A SMALL SCALE THERMOSYPHON HEAT EXCHANGER(U) RENSSELAER 1/1
POLYTECHNIC INST TROY NY DEPT OFCCHEMICAL ENGINEERING
M SUJANANI ET AL. 01 NOV 86 AFOSR-RR-87-0128
UNCLASSIFIED AFOSR-84-0306 F/G 20/13 NL

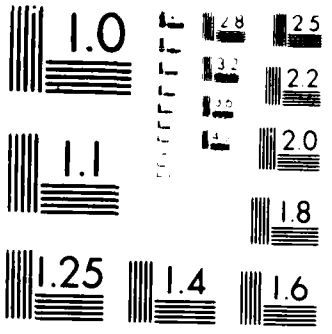
1.0
1.1
1.25
1.4
1.6
1.8
2.0
2.2
2.5

(2)

AD-A177 078

DTIC SELECTE FEB 05 1987 S D

ORT DOCUMENTATION PAGE

1a. REPORT SECURITY CLASSIFICATION: Unclassified	1b. RESTRICTIVE MARKINGS: None
2a. SECURITY CLASSIFICATION AUTHORITY	3. DISTRIBUTION/AVAILABILITY OF REPORT: Distribution unlimited; approved for public release
2b. DECLASSIFICATION/DOWNGRADING SCHEDULE	
4. PERFORMING ORGANIZATION REPORT NUMBER(S)	5. MONITORING ORGANIZATION REPORT NUMBER(S): AFOSR-TR- 87-0128
6a. NAME OF PERFORMING ORGANIZATION: Rensselaer Polytechnic Inst. Dept. of Chemical Engineering	6b. OFFICE SYMBOL (If applicable):
7a. NAME OF MONITORING ORGANIZATION: Air Force Office of Scientific Research	
6c. ADDRESS (City, State and ZIP Code): Troy, NY 12180-3590	7b. ADDRESS (City, State and ZIP Code): Bolling AFB DC 20332-6448
8a. NAME OF FUNDING/SPONSORING ORGANIZATION: Air Force Office of Scientific Res	8b. OFFICE SYMBOL (If applicable): AFOSR/NA
	9. PROCUREMENT INSTRUMENT IDENTIFICATION NUMBER: AFOSR-84-0306
8c. ADDRESS (City, State and ZIP Code): Bolling Air Force Base, Washington, D.C. 20332	10. SOURCE OF FUNDING NOS.

PROGRAM ELEMENT NO.	PROJECT NO.	TASK NO.	WORK UNIT NO.
61102F	2308	A1	

11. TITLE (Include Security Classification): A Small Scale Thermosyphon Heat Exch...

12. PERSONAL AUTHOR(S): Sujanani, Manoj; Kiewra, Edward William; Wayner, Peter Charles Jr.

13a. TYPE OF REPORT	13b. TIME COVERED	14. DATE OF REPORT (Yr., Mo., Day)	15. PAGE COUNT
Presentation	FROM 86/1/1 TO 86/11/1	86/11/1	6

16. SUPPLEMENTARY NOTATION: To be presented at 6th International Heat Pipe Conference, Grenoble, France, May 25-29, 1987

17. COSATI CODES		
FIELD	GROUP	SUB. GR.
20	13	
10	01	

18. SUBJECT TERMS (Continue on reverse if necessary and identify by block number): Heat Transfer; Interfacial Phenomena; Electronic Cooling; Heat Pipes; Thermosyphon

19. ABSTRACT (Continue on reverse if necessary and identify by block number)

A Small Scale Thermosyphon Heat Exchanger

A small circular heat transfer cell was used to study the cooling of a disc heat source by a thin evaporating liquid film. This small scale thermosyphon is a thermal spreader and a passive heat sink in that the interfacially induced liquid flow rates are controlled by the heat input. To determine the pressure gradient, the evaporating liquid film profile is "viewed" interferometrically through the objective of a microscope which is equipped with a scanning microphotometer to measure its thickness profile. Experimental data for the operation of the cooling device with pure fluids (n-alkanes, Freon 113) are presented. The combined use of an evaporating thin circular film in the shape of an extended meniscus and condensation within a small volume gives an effective heat spreader for the cooling of small electronic heat sou-ces. The surface heat flux and heat transfer coefficient can be enhanced by increasing the interline-length/area ratio.

20. DISTRIBUTION/AVAILABILITY OF ABSTRACT	21. ABSTRACT SECURITY CLASSIFICATION
UNCLASSIFIED/UNLIMITED ☒ SAME AS RPT. ☐ DTIC USERS ☐	Unclassified

22a. NAME OF RESPONSIBLE INDIVIDUAL	22b. TELEPHONE NUMBER (Include Area Code)	22c. OFFICE SYMBOL
Julian M Tishkoff	(202) 767-4935	AFOSR/NA

DD FORM 1473, 83 APR — EDITION OF 1 JAN 73 IS OBSOLETE.

UNCLASSIFIED
SECURITY CLASSIFICATION OF THIS PAGE

For presentation at the Sixth International Heat Pipe Conference,
Grenoble, France, May 25-29, 1987

A SMALL SCALE THERMOSYPHON HEAT EXCHANGER

Sujanani, M., Kiewra, E.W., and Wayner, P.C., Jr.

Department of Chemical Engineering
Rensselaer Polytechnic Institute
Troy, NY 12180-3590

ABSTRACT

A small circular heat transfer cell was used to study the cooling of a disc heat source by a thin evaporating liquid film. This small scale thermosyphon is a thermal spreader and a passive heat sink in that the interfacially induced liquid flow rates are controlled by the heat input. To determine the pressure gradient, the evaporating liquid film profile is "viewed" interferometrically through the objective of a microscope which is equipped with a scanning microphotometer to measure its thickness profile. Experimental data for the operation of the cooling device with pure fluids (n-alkanes, Freon 113) are presented. The combined use of an evaporating thin circular film in the shape of an extended meniscus and condensation within a small volume gives an effective heat spreader for the cooling of small electronic heat sources. The surface heat flux and heat transfer coefficient can be enhanced by increasing the interline-length/area ratio.

NOMENCLATURE

a	= radius ratio
A	= area (m^2)
$\bar{A}$	= modified Hamaker Constant (N-m)
B	= London-van der Waals Constant ($N-m^2$)
h	= heat transfer coefficient (W/m^2-K)
h_{fg}	= heat of vaporization (kJ/kg)
k	= thermal conductivity of silicon (W/m-K)
K	= curvature (1/m)
L	= order of fringe
M	= constant in Equation (4)
$\dot{m}_e$	= evaporative mass flux (kg/m^2-sec)
P	= pressure (N/m^2)
P_v	= vapor pressure (N/m^2)
q_e	= local heat flux (kW/m^2)
Q	= heat flow rate (Watts)
r	= radius (m)
R	= resistance to heat transfer (°C/Watts)
$\bar{R}$	= dimensionless radius
t	= thickness of wafer substrate (m)
T	= temperature (°C)
U	= overall heat transfer coefficient (W/m^2-K)
v	= velocity (m/sec)

Greek

δ	= film thickness (m)
λ	= wavelength of light (548 nm)
n	= refractive index of liquid
θ	= dimensionless temperature = $(T-T_\infty)/(T_i-T_\infty)$
ν	= kinematic viscosity (m^2/sec)
μ	= viscosity (kg/m-sec)
τ	= shear stress (N/m^2)
Γ	= mass flow rate (kg/sec)
ρ	= density (kg/m^3)
σ	= surface tension (N/m)

Subscripts

b	= bottom
c	= cavity (r_c = 12.5 mm)
dry	= dry cell
f	= fluid
i	= edge of heater (r_i = 2.5 mm)
ℓ	= liquid
o	= edge of silicon substrate (r_o = 38 mm)
r	= radial component
t	= top
vac	= vacuum
z	= axial component
θ	= angular component

INTRODUCTION

In order to optimize the performance of a thermosyphon and/or a heat pipe, the following phenomena require evaluation and optimization: (i) fluid flow with evaporation in ultra-thin films over a small surface area in which interfacial forces predominate; (ii) convection of the resulting vapor; (iii) condensation over a large surface area; and (iv) the return flow of the condensate to the zone of evaporation. In this paper we are primarily concerned with the stability and the heat transfer characteristics of evaporating thin films which are two of the critical areas to study.

We present results concerning the design and use of the small scale thermosyphon shown in Figure (1). This particular design has both applied and experimental attributes. Using the phenomena associated with interfacial forces and the mechanisms of evaporation-condensation in a heat exchanger, it should be possible to transform the high heat flux at the surface of a small disc heat source to a lower heat flux over a larger area with a minimum temperature difference penalty. As an experimental tool, the thermosyphon presented in Figure (1) can be used to study and thereby optimize the basic mechanisms of heat, mass, and momentum transfer in an environment designed to enhance natural evaporative cooling due to both body and interfacial forces.

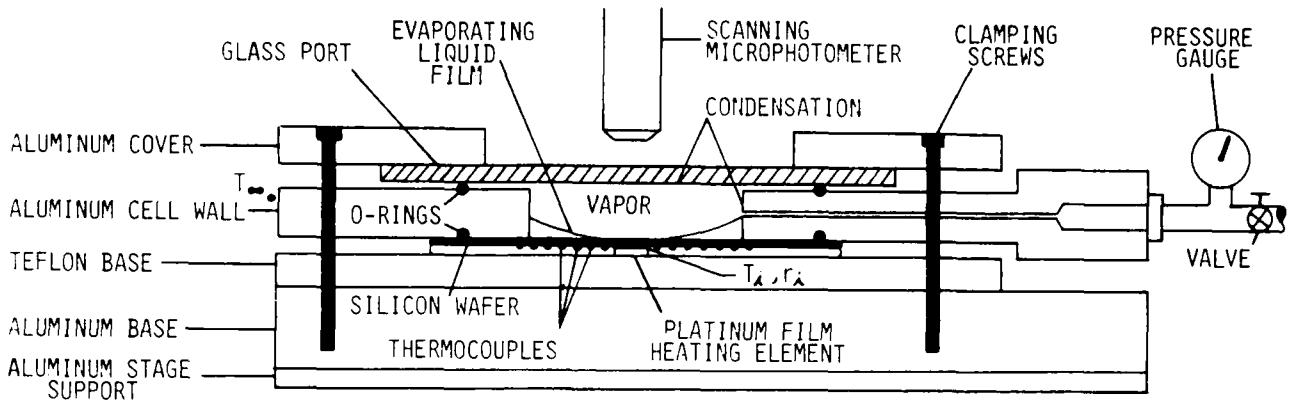

Fig. 1 Cross-Sectional View of the Small Scale Circular Thermosyphon

We note that the results presented below are concerned with a single circular contact line. Therefore, the heat fluxes based on the larger substrate area are small. However, the number and length of interlines on the substrate can be enhanced and therefore the heat flux can be improved by milling, in a designed way, multiple microchannels on the surface. On the other hand, the apparent heat flux can be increased by decreasing the substrate area relative to the interline length. Using a surface modified by capillary grooves and fins, Barthelemy, et al. [1] have demonstrated high heat fluxes. Herein we have reduced the internal surfaces to a simple smooth film which can be studied using first principles. These "calibration studies" will then be used in future research to design enhanced surfaces for high performance compact heat exchangers.

EXPERIMENTAL EQUIPMENT AND PROCEDURE

The small circular heat cell illustrated in Figure (1) was used to study the cooling of a disc heat source by a thin evaporating liquid. The substrate of the cell is a single crystal of electronic grade silicon that is 7.6×10^{-2} m in diameter and 4×10^{-4} m thick. The heat source is a resistance heater in the form of a thin platinum compound film with an inherent resistance of about 100 ohms. This S-shaped heater was inscribed in a circle of diameter 5×10^{-3} m on the backside of the substrate, thus providing intimate contact with the silicon. The choice of using a single crystal silicon substrate was governed by its high degree of surface uniformity, high reflectivity and well-known optical and physical properties. Further, the processing of small scale temperature sensors and micro-grooves planned for future studies, would be possible with a single-crystal silicon wafer as the substrate. Uses in the cooling of VLSI circuits on silicon are also of interest. The substrate was epoxied to a teflon base and the outer walls of the cell were constructed of polished aluminum. A pyrex glass port covered the cell and allowed an unobstructed view of the heat transfer chamber, base and fluid. Two O-rings made of a material which was tested for inertness with the fluids provided a static seal of the chamber. For the alkanes, Buna-N was found to be the best suited material. The cell pressure was monitored and controlled using a vacuum port. An injection port was also built into the cell to ensure better control over fluid volume in the cell.

To measure the integral temperature distribution along the silicon wafer, 0.08 mm diameter, type K thermocouples were attached at intervals of 1 mm (in the radial direction) from r = 3 mm to r = 12 mm, along the bottom of the substrate. Due to the low thermal conductivity of the glue, it was essential to ensure complete and proper contact of the thermocouple sensor bob with the backside of the substrate. Since the thermal conductivity of silicon is high (k = 120 W/m-K), the temperature difference across a thin wafer is small.

The cell was assembled and connected through the use of four clamping screws. Cleanliness is critical to our studies as even a small amount of impurities can radically change the film profile. Hence all the cell parts were immersed in absolute, 200 proof ethanol and dried at 100°C in a dust-free oven. The silicon substrate was etched with hydroflouric acid and rinsed with ethanol, acetone and the working fluid, in that order, before being used. The glass port was cleaned in chromic acid, washed with ethanol and also dried in the oven.

The cell was evacuated by means of a vacuum pump to a pressure of below 100 N/m^2. The experiments were done when it had been established that the vacuum level remained constant over a period of at least 12 hrs. The power input to the cell was controlled by varying the voltage across the heater, and temperature data were recorded for power inputs of 0.5, 1,2,3, and 4W. To reduce the resistance due to natural convection, a fan forced air over the glass top during the experiments.

The working fluid (decane/hexane/pentane/Freon 113) was then introduced by opening both the injection valve and the vacuum valve to the cell. The valve to the pressure gauge was closed while the fluid was being injected. When the valve was reopened the pressure rose to read slightly above the vapor pressure of the fluid at room temperature. This difference was attributed to the presence of a small amount of dissolved air in the liquid. It is planned to 'degas' the liquid to eliminate this dissolved air in our final studies. The volume of the fluid injected was controlled so as to get a thin film within the operating range of power input.

The temperature profiles were determined at the various power inputs for the different working fluids. These were compared to the temperature profiles obtained when there was no fluid in the cell.

The thickness profile was measured using a scanning microphotometer [2]. The fringes observed due to the constructive and destructive interference of light are as shown in Figure (2).

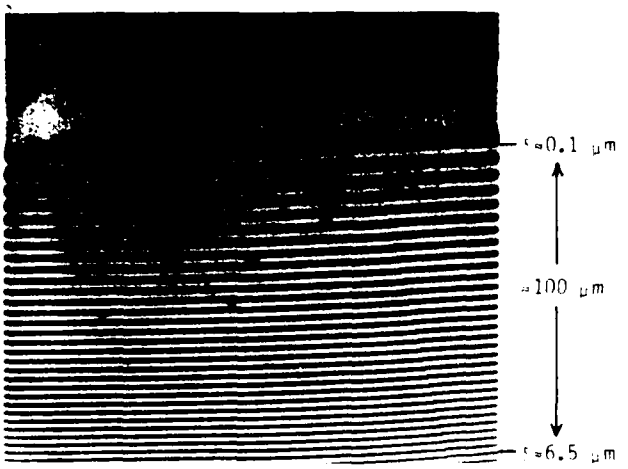

Fig. 2 Interference Fringes for Decane at 1 W

When these fringes were scanned using a photometer, the thickness profile ε vs. r can be calculated from

$$\varepsilon = \frac{(2L+1)\lambda}{4n} \quad , \quad L = 0,1,2,\ldots \qquad (1)$$

This thickness profile was used to determine the fluid flow and the heat transfer rate in the interline region using the momentum balance model.

THERMAL ANALYSIS

The analytical solution for the temperature profile was obtained by considering a circular silicon plate of 76 mm diameter and 0.4 mm in thickness, being heated in a central circular region of 5 mm in diameter, and cooled by heat loss to the surroundings through different mechanisms on the top and bottom surfaces with a constant value of the overall heat transfer coefficient, U. The boundary conditions for the solution were

i) $T = T_i$ at r = 2.5 mm (edge of heater)

ii) $T = T_\infty$ at $r = \infty$

iii) $\frac{dT}{dr} = 0$ at r = 38 mm (edge of silicon wafer)

T_i was obtained experimentally by extrapolating the profile to r = 2.5 mm. T_∞ was obtained experimentally as the temperature of a thermocouple in the air beside the cell. It was also confirmed experimentally that (dT/dr) at the end of the silicon wafer was very small.

A heat balance gives

$$Q_r = Q_{r+dr} + U \cdot 4\pi r dr (T - T_\infty) \quad , \text{ or} \qquad (2)$$

$$\frac{d}{dr}\left(r \frac{dT}{dr}\right) = \frac{2Ur}{kt}(T - T_\infty) \qquad (3)$$

To non-dimensionalize the problem we used

$$\bar{R} = \frac{r}{r_o} \; ; \; \theta = \frac{T - T_\infty}{T_i - T_\infty} \; ; \; M = \sqrt{2Ur_o^2/kt} \qquad (4)$$

Using these definitions in equation (3) gives

$$\frac{d}{d\bar{R}}\left(\bar{R} \frac{d\theta}{d\bar{R}}\right) = M^2 \bar{R}\theta \qquad (5)$$

The solution to this standard hyperbolic Bessel differential equation of order zero, is given by [4,5]

$$\theta(\bar{R}) = \frac{K_1(M)I_0(M\bar{R}) + I_1(M)K_0(M\bar{R})}{I_0(Ma)K_1(M) + I_1(M)K_0(Ma)} \qquad (6)$$

where $a = (r_i/r_o)$, and

I_k = Modified Bessel function of the first kind of order 'k'

K_k = Modified Bessel function of the second kind of order 'k'

Non-dimensional θ vs. $\bar{R}$ plots were thus obtained, using a constant value of U = 25, 50, and 100 W/m^2-K. Representative plots of the experimental data for the four working fluids at power inputs of Q = 1 W and Q = 4 W are shown in Figures (3) and (4). We note that since the definition of U is arbitrary (due to the area under consideration and definition of ΔT), these values mainly are of relative importance.

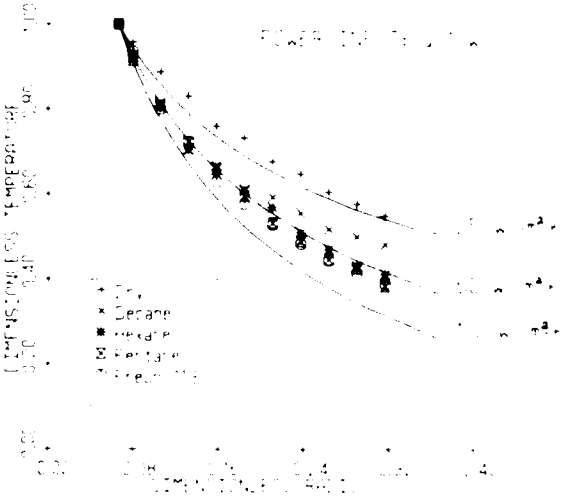

Fig. 3 Temperature vs. Radius for Q = 1W

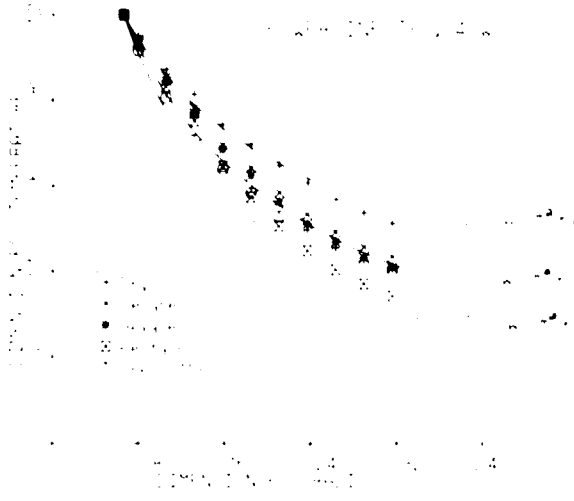

Fig. 4 Temperature vs. Radius for Q = 4W

ANALYSIS OF RESISTANCES TO HEAT TRANSFER

To optimize the performance of the thermosyphon we need to evaluate the various factors which contribute to the overall resistance to heat transfer. The basic processes occurring are: (i) fluid flow with evaporation in ultra-thin films over a small surface area in which interfacial forces predominate; (ii) conduction through the liquid and vapor; (iii) convection of the vapor (diffusion is important if non-condesibles are present); (iv) condensation over a large surface area; (v) return flow of the condensate to the zone of evaporation; and (vi) all other resistances due to conduction through the solid and convection from the glass port to the surroundings.

If no non-condensibles are present, then the resistance due to (iii) is negligible. We note that due to some dissolved air in the liquid and possible minute leaks in the vacuum (5 N/m^2-hr) we have only minimized this resistance experimentally. To completely separate the various resistances is not possible at present due to coupling. Data from microthermistors is needed for this purpose. However, we can divide the resistances into two groups: (i) those resistances which change with the physical properties of the fluid, (e.g., conduction through liquid, convection through vapor, fluid flow and return flow of condensate); and (ii) those resistances which do not change when we change the fluid, (e.g., conduction through substrate, glass, and metal, and external convection, etc.).

Using a vacuum in the cell, the resistance offered by the solid part of the cell can be isolated because the resistance in the cavity tends to infinity. If we hypothesize that these two resistances act in parallel, we have

$$\frac{1}{R} = \frac{1}{R_f} + \frac{1}{R_c} \tag{7}$$

In an evacuated cell, $R_f = \infty$, and therefore $R_{vac} = R_c$. Now if R_{vac} is assumed constant when R_f is varied then,

$$R_f = \frac{R\,R_{vac}}{R_{vac} - R} \tag{8}$$

The fluid resistance in the cavity is a function of various resistances due to fluid flow, condensate return, etc. However we expect that the resistance due to convection will be predominantly a function of vapor pressure. We note that the resistance between the solid and surrounding air is small due to the large surface area. Based on previous theoretical analysis [6] other factors which may contribute to R_f and the final maximum heat flux for one interline are $(\sigma h_{fg}/\nu)$ and $(\overline{A}h_{fg}/\ell)$. However these are less important in the current studies because the size of the dry spot can change.

In this study we can analyze the effect of variation of vapor pressure on the overall process for a homologous series of alkanes. Defining

$$P = \frac{1}{UA} \tag{9}$$

$$A = A_t + A_b = 2\pi r_c^2 \tag{10}$$

where A is the total area for heat transfer, U is the overall heat transfer coefficient and 'r_c' is the radius of the cavity (r_c = 12.5 mm).

Then by the approximate values of 'U' obtained from Fig. (4) for each case, we can get R_f by using Equation (8). We note that this is equivalent to relating the overall heat transfer coefficient to the individual top and bottom heat transfer coefficients as

$$U = \frac{h_t + h_b}{2} \tag{11}$$

For the dry plate $h_t = 0$ and therefore

$$U_{dry} = \frac{h_b}{2} \tag{12}$$

If 'h_b'is assumed constant for all fluids then

$$h_t = 2(U - U_{dry}) \text{ , and} \tag{13}$$

$$R_f = \frac{1}{h_t \cdot \pi r_c^2} \tag{14}$$

Equation (14) is exactly equivalent to Eqn. (8). Thus h_t was calculated using equation (13), and h_t vs. P_v is ploted in Figure (5) where P_v is the vapor pressure of the fluid evaluated at $T = (T_i + T_\infty)/2$.

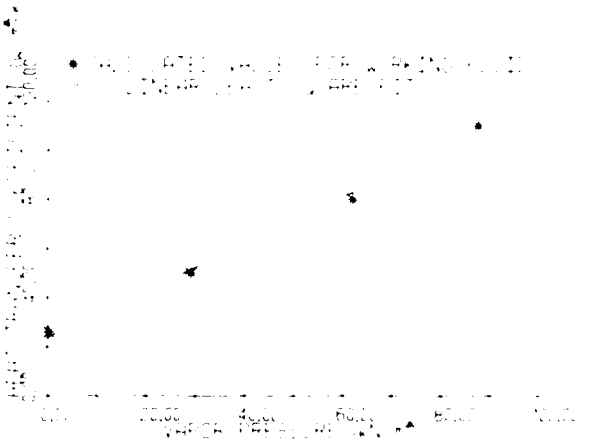

Fig. 5 Heat Transfer Coefficient vs. Vapor Pressure

FLUID FLOW IN AN EVAPORATING FILM AND THE MOMENTUM BALANCE MODEL

From a basic analysis of fluid flow, we find that the flow is symmetric with respect to θ and $V_\theta = 0$. Using the equation of continuity and the Navier-Stokes equations while neglecting v_z and inertia terms, the following simplified equation can be written for the r-direction

$$\mu \frac{\partial^2 v_r}{\partial z^2} = \frac{\partial p_\ell}{\partial r} \tag{15}$$

Equation (15) can be solved for the velocity distribution using the boundary conditions

$$z = 0,\ v_r = 0 \text{ (no slip)} \tag{16}$$

$$z = \delta,\ -\tau_{rz} = \mu \frac{\partial v_r}{\partial z} = \frac{d\sigma}{dr} \tag{17}$$

The second boundary condition has a significant effect on the velocity distribution because of the effect of gradients in temperature and con-

centration (even if a minute amount of impurity is present).

Using equations (15) - (17), we obtain

$$v_r = \frac{1}{\mu}\frac{\partial p_i}{\partial r}\left[\frac{z^2}{2} - \delta z\right] + \frac{z}{\mu}\frac{d\sigma}{dr} \qquad (18)$$

The normal pressure difference at the liquid-vapor interface may be written as

$$p_i = p_v - \sigma K - \frac{B}{\delta^4} \qquad \delta > 10 \text{ nm} \qquad (19)$$

in which the curvature may be approximated as

$$K = \frac{1}{r} + \frac{d^2\delta}{dr^2}\left[1 + \left(\frac{d\delta}{dr}\right)^2\right]^{-3/2} \qquad (20)$$

and B/δ^4 accounts for the disjoining pressure [7]. For $\delta < 10$ nm, A/δ^3 would replace B/δ^4. The mass flow rate is

$$\dot{m} = \int_0^\delta v_r \cdot 2\pi r \, dz \qquad (21)$$

Using equations (18-21), we get

$$\dot{m} = \frac{2\pi r}{\mu}\left[\frac{\delta^3}{3}\left(\sigma\frac{dK}{dr} - \frac{4B}{\delta^5}\frac{d\delta}{dr}\right)\right] + \left[\frac{\delta^2}{2}\left(K\sigma + 1.5\frac{d\sigma}{dr}\right)\right] \qquad (22)$$

where

$$\frac{d\sigma}{dr} = \frac{d\sigma}{dT}\cdot\frac{dT}{dr} \qquad (23)$$

In our experiments, (dT/dr) is negative and $(d\delta/dr)$ is positive for a pure fluid. Thus the temperature induced surface shear stress would hinder fluid flow towards the contact line. However, we note that [2,8] a small impurity affects the fluid flow to a great extent therefore if the impurity has a lower vapor pressure and a higher surface tension, a surface tension gradient due to a concentration gradient can significantly enhance flow towards the contact line. Surface tension effects are very complicated.

The evaporative mass flux may now be obtained by using Equation (24) and (25).

$$\dot{m}_e = -\frac{1}{2\pi r}\frac{d\dot{m}}{dr} \qquad (24)$$

$$\dot{m}_e = -\frac{1}{\mu r}\left[\frac{\delta^3}{3}\cdot\frac{d\sigma}{dr}\cdot\frac{d\delta}{dr} + \frac{4B}{3\delta^2}\frac{d\delta}{dr} + \frac{\delta^3}{3}\sigma K\frac{d\delta}{dr} + \frac{\delta^2}{2}\frac{d\sigma}{dr}\right]$$

$$- \frac{1}{\mu}\left[\delta^2\cdot\frac{d\sigma}{dr}\frac{d\delta}{dr} + \frac{2\delta^3}{3}\frac{d\sigma}{dr}\frac{d\delta}{dr} + \frac{\delta^3}{3}\sigma\frac{d^2\sigma}{dr^2}\right]$$

$$- \frac{4B}{3\delta^2}\frac{d^2\delta}{dr^2} + \frac{8B}{3\delta^3}\left(\frac{d\delta}{dr}\right)^2 + K\sigma^2\frac{d\delta}{dr}\frac{d\delta}{dr}$$

$$+ \frac{\delta^3}{3}\sigma\frac{d^2\sigma}{dr^2} + \sigma\frac{d\delta}{dr}\frac{d\sigma}{dr} + \frac{\delta^2}{2}\frac{d^2\sigma}{dr^2} \qquad (25)$$

The local value of the heat flux is then

$$q_e'' = \dot{m}_e h_{fg} \qquad (26)$$

For the purpose of data analysis, we make the following assumptions: (i) (dT/dr) is almost constant in the interline region (then, by using the pure fluid approximation, $(d\sigma/dr) = (d\sigma/dT)\cdot(dT/dr)$ = constant); and (ii) $(d\delta/dr)$ is very small and hence the curvature may be represented as

$$K = \frac{1}{r} + \frac{d^2\delta}{dr^2} \qquad (27)$$

Then by fitting our experimental δ vs. r profile to a sixth degree polynomial in a least square sense (as in Figure (6)), we can derive the mass flow rate and the local heat flux using Equations (22,25,26). These profiles are shown in Figure (7).

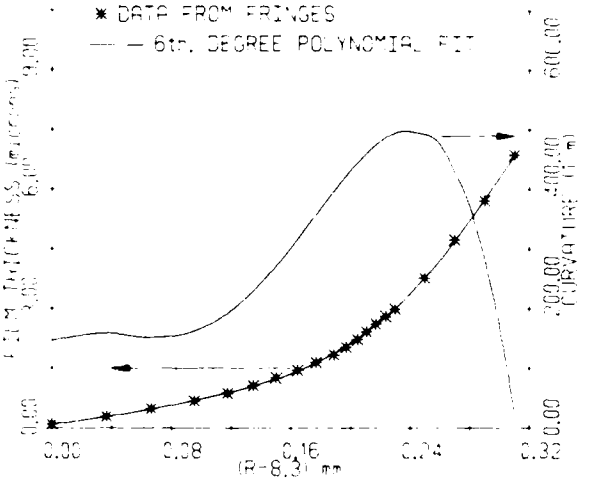

Fig. 6 Film Thickness and Curvature vs. Radius (Radius of dry spot = 8.3 mm)

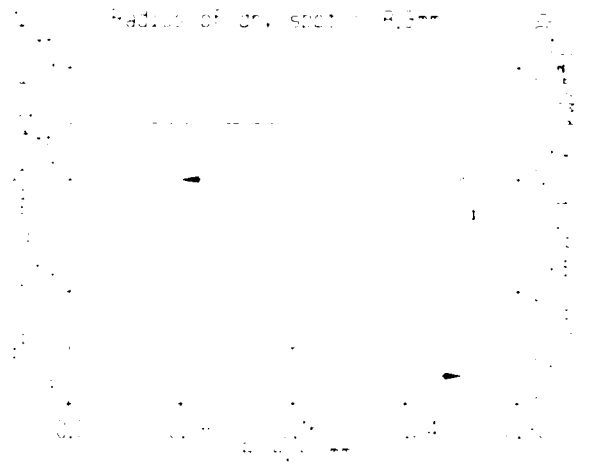

Fig. 7 Mass Flow Rate and Local Heat Flux vs. Radius

From the fluid flow analysis based on the experimental film thickness vs. radius plot derived from the recorded fringe pattern, we find that the present model which does not take into account any shear stress due to a concentration gradient (as might arise due to any impurity) predicts a very small amount of fluid flow away from the contact line in a small region at the beginning of the interline and subsequent substan-

tial flow towards the contact line. We note that in our previous studies we have found that flow towards the contact line is always present and is a stable situation. We therefore do suspect impurities in our feed fluid, which though in a very small concentration (<0.01%) could affect the profile. Indeed at high heat fluxes, instability or breaking up of the interline was observed as is shown in Figure (8).

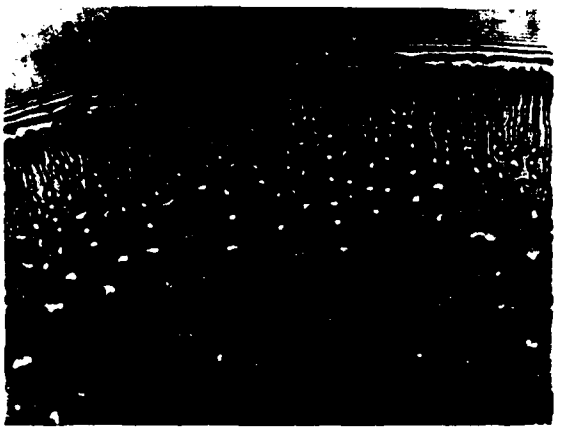

Fig. 8 Instability of Decane at Q = 3W

EXPERIMENTAL RESULTS

Comparison between the temperature profiles generated by the analytical solution to the modified Bessel's equation and the experimental temperature profiles shows that the heat transfer coefficient follows the trend $U_{pentane} > U_{Freon\ 113} > U_{hexane} > U_{decane} > U_{dry}$.

This is expected because as the vapor pressure of the fluid gets higher, the resistance decreases (again, see Figure 5).

Average values for the overall heat transfer coefficient and h_t for the various fluids are

$U_{dry} = 25\ W/m^2\text{-}K$

$U_{decane} = 38\ W/m^2\text{-}K; \quad h_{t_{decane}} = 26\ W/m^2\text{-}K$

$U_{hexane} = 50\ W/m^2\text{-}K; \quad h_{t_{hexane}} = 50\ W/m^2\text{-}K$

$U_{pentane} = 80\ W/m^2\text{-}K; \quad h_{t_{pentane}} = 110\ W/m^2\text{-}K$

$U_{Freon\ 113} = 65\ W/m^2\text{-}K; \quad h_{t_{Freon\ 113}} = 80\ W/m^2\text{-}K$

We note that the extent of the interline region is only a fraction of a millimeter. To measure the physical parameters needed to characterize and model heat transfer processes on a miniature scale, we need to employ devices whose dimensions are on the order of the process itself. To control and optimize the physical parameters (e.g., film thickness, temperature distribution, and concentration) we need devices whose sensing area is quite small and sensitive. Such devices are being fabricated using miniature solid state processing techniques, e.g., photolithography, making patterns by selective etching.

Since it is expected that the overall heat sink capability of the interline is proportional to the length of the interline, enhancing the interline length through surface modification should improve the heat sink capability of the thermosyphon. We are considering the incorporation of this variable in our future studies.

CONCLUSIONS

i) An effective thermosyphon for the cooling of a disc heat source was designed.

ii) Integral temperature profiles for decane, hexane, pentane and Freon 113 were obtained.

iii) The resistance to heat transfer was found to decrease with increasing vapor pressure of the fluid.

iv) A preliminary analysis of the fluid flow suggests that the interfacial shear stresses due to temperature and concentration gradients are critical in determining the fluid flow rate.

v) The heat sink capability may be increased by increasing the interline length by making microchannels.

ACKNOWLEDGEMENTS

The authors would like to thank Mr. C.J. Parks for his valuable discussions and help with the computations.

This material is based on work supported by the Air Force Office of Scientific Research, Air Force System Command, USAF, under Grand Number AFOSR-84-0306. The U.S. Government is authorized to reproduce and distribute reprints for governmental purposes notwithstanding any copyright notation. Any opinions, findings, and conclusions or recommendations expressed in this publication are those of the authors and do not necessarily reflect the view of the U.S. Air Force Office of Scientific Research.

REFERENCES

[1] BARTHELEMY, P.R., JACOBSON, D., and RABE, D., "Heat pipe mirrors for high power lasers," Proceedings of the 3rd Int. Heat Pipe Conference, May 22-24, 1978, Palo Alto, CA, pp. 63-70.

[2] COOK, R., TUNG, C.Y. and WAYNER, P.C., JR., "Use of scanning microphotometer to determine the evaporative heat transfer characteristics of the contact line region," ASME Journal of Heat Transfer, Vol. 103, 1981, pp. 325-330.

[3] KIEWRA, E.W. and WAYNER, P.C., JR., "A small scale thermosyphon for the immersion cooling of a disc heat source," Heat Pipe and Immersion Cooling of Microelectronics Session, AIAA/ASME Thermophysics and Heat Transfer Conference, Boston, June 1986, pp. 77-82.

[4] MYERS, G.E., "Analytical Methods in Conduction Heat Transfer, Chap. 2, McGraw-Hill, NY, 1971.

[5] FLUGGE, W., "Four place tables of transcendental functions," McGraw-Hill, NY, 1954.

[6] WAYNER, P.C., JR., "The effect of the London-van der Waals dispersion force on interline heat transfer," ASME Journal of Heat Transfer, Vol. 100, Feb. 1978, pp. 155-159.

[7] WAYNER, P.C., JR. and PARKS, C.J., "Effect of liquid composition on enhanced flow due to surface shear in the contact line region: constant vapor pressure boundary condition," Multiphase Flow and Heat Transfer-HTD, Vol. 47, ASME, Editors V.K. Dhir, J.C. Chen and O.C. Jones, 1985, pp. 57-63.

[8] WAYNER, P.C., JR., TIRUMALA, M., TUNG, S.C.Y., and YANG, J.H., "Fluid flow in a contact line region of a mixture of alkanes: 98% Hexane and 2% Octane," AIAA 18th Thermophysics Conference, Montreal, Canada, June 1-3, 1983.

END

4-[redacted]-87

DTIC